

Ultrasonic Monitoring of Capillary Porosity Evolution and Strength Gain in Hydrating Cement Pastes

K.V.L. Subramaniam

Abstract An ultrasonic test procedure for determining the capillary porosity in hydrating cement paste is presented. The response of hydrating cement paste through setting is monitored using horizontally polarized shear waves (SH). Changes in the ultrasonic signal through setting are related with changes in the porosity and stiffness of an equivalent water-filled poroelastic material, which provides identical acoustic impedance. The porosity obtained from the ultrasonic measurements, is identical to capillary porosity obtained from the conventional thermo-gravimetric analysis. A unique relationship between capillary porosity and compressive strength is established for hydrating cement pastes.

Keywords Capillary porosity • Cement paste • Compressive strength • Hydration • Shear waves • Ultrasound

Introduction

Accurate determination of the changes in the microstructure of hydrating cement through setting, and early strength gain of the material has remained a major experimental challenge. Conventional methods for probing the microstructure are not conducive to studying changes in microstructure in the first few hours after casting because (a) sample preparation procedures either alter or disturb the microstructure [1] and (b) changes in microstructure occur on a time scale that is an order of magnitude faster than the time required for sample preparation [2]. Our current understanding of changes in the microstructure during setting obtained from the computer simulation models indicates that initially starting from a weak skeleton comprised

K.V.L. Subramaniam (✉)

Department of Civil Engineering, Indian Institute of Technology, Hyderabad, INDIA
e-mail: kvl@iith.ac.in

of loosely connected cement grains within the fluid medium, the products of hydration link up to provide a continuous network of solid within the fluid filled space. The emergence of a continuous solid phase within the fluid medium has been identified as the percolation threshold [3,4]. Following percolation threshold, setting behavior is initiated in the cement paste. Through setting, as the products of hydration form within the fluid-filled spaces of cement paste, a network of pores and a pore structure develops.

The primary focus of the research presented here is to assess changes in the microstructure associated with porosity in hydrating cement paste through the setting process from ultrasonic measurements. The method measures reflection of SH waves at the surface of hydrating cement paste. A poroelastic equivalent material for hydrating cement paste is derived by matching the measured reflections response with changes in the poro-elastic parameters.

Experimental Program

The test program consisted of the following measurements: (a) ultrasonic SH wave reflection; (b) Thermogravimetric (TG) weight. Cement paste samples with water-to-cement ratios equal to 0.35, 0.45 and 0.5, were evaluated.

Ultrasonic test procedure

A schematic diagram of the experimental setup for oblique ultrasonic wave reflection measurement is shown in Fig. 1. The test probe consists of ultrasonic transducer(s) attached to a buffer plate made of fused quartz, which is in contact with the hardening cement paste. Multiple pairs of transducers (T and R) with a center frequency of 1 MHz were mounted on precisely machined faces at matched angles with respect to the vertical to generate SH waves. Wave reflection at the fused-quartz/cement paste interface was monitored at 0, 50 and 60 degree angles of incidence. The amplitude reflection factor, $r(1)$, which gives the decrease in the amplitude of a 1 MHz incident signal after reflection, was obtained using the self-compensating technique [2,5].

TG weight loss measurements

The evaporable and the non-evaporable water contents within the hydrating cement paste at different ages were measured. Weights of the samples were recorded after drying the sample at 105 °C before ramping the temperature to 1000 °C at 10 °C/ minute. During the heating, the furnace was purged with nitrogen gas.

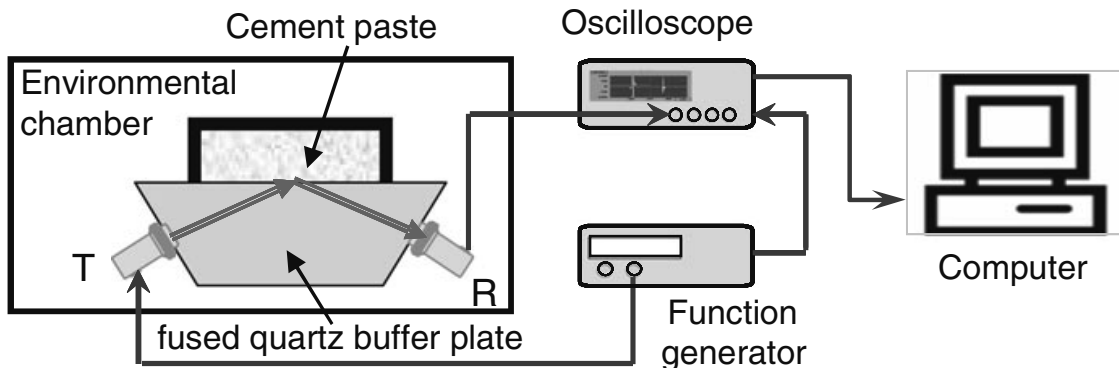


Fig. 1 Schematic Diagram of Test Setup for Ultrasonic Measurements

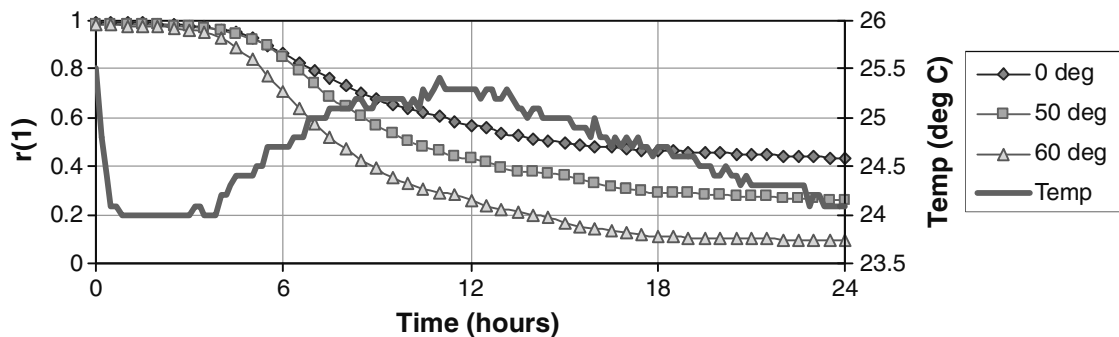


Fig. 2 Temperature and $r(1)$ as a function of age after mixing

Analysis of Data

Changes in $r(1)$ and temperature for cement paste with w/c equal to 0.5 are shown in Fig. 2. Immediately after mixing, the measured $r(1)$ for the three angles of incidence are close to 1.0, suggesting that a significant portion of the incident wave energy is reflected at the quartz-cement paste interface. The increase in temperature after the dormant period signals the beginning of the acceleration stage, which is followed by the slow decrease in temperature in the deceleration stage. Starting from a gradual rate of change at the end of the dormant period, the rate of change in $r(1)$, corresponds well with the reaction rate indicated by the temperature measurements.

The measured changes in the $r(1)$ can now be interpreted in terms of the expected result from the reflection of an SH wave at the interface between an elastic and a poroelastic material. In the poroelastic idealization, the hydrating cement paste is assumed to be comprised of a water-filled porous skeleton. The material of the skeleton is assumed to be homogenous and isotropic. The exact magnitude of change in amplitude of an incident SH wave $r(f)$ after reflection can be obtained considering dynamic equilibrium and displacement continuity at the interface [5-7]. Changes in

the amplitude and phase of the wave following reflection from the poroelastic material can be symbolically expressed as [see Refs 5 for details]

$$R_s = r(f)e^{i\Phi} = R_s(\rho_e, E_e, v_e, \rho_s, \rho_f, K_f, \mu_b, \beta, \eta, a, c, \kappa, \delta_\mu) \quad (1)$$

where ρ_e , E_e , and v_e are the density, the Young's modulus and the Poisson's ratio of the fused quartz, β is the porosity (assumed to be isotropic), ρ_s and ρ_f are the solid and fluid mass densities, respectively, η is the fluid viscosity, and κ is the coefficient of permeability of the porous frame, a is the pore diameter, c is the tortuosity coefficient, μ_b is the shear modulus of the skeletal frame (under drained conditions), K_f is the bulk modulus of the pore fluid. For the porous medium, the dynamic shear modulus of the skeletal frame is given as

$$\bar{\mu}_b = \mu_b(1 + \delta_\mu i) \quad (2)$$

where δ_μ is the loss factor, which is usually a small number in the range of 0.11 – 0.17 [7,8]. In Equ. (2), the internal system variables of the fluid filled porous medium are shown in grey.

When applied to the case of hydrating cement paste, some simplifications can be introduced to the expression for R_s , assuming the hydrating cement paste is a water-filled porous skeleton, $K_f = 2.0 \times 10^9$ Pa, and the viscosity $\eta = 1.0 \times 10^{-3}$ Kg/ms. Further, changes in density of the hydrating cement paste with age (on account of chemical shrinkage) can be considered to produce insignificant changes in the bulk density of the material. Thus considering the hydrating cement material to be composed of two components, the porous skeleton (made up of cement grains and products of hydration) and water, a simple relation can be obtained considering

$$\rho_{bulk} = (1 - \beta)\rho_s + \beta\rho_f \quad (3)$$

where, ρ_{bulk} is the density of the cement paste. ρ_{bulk} can be considered to be constant through the hydration process. The ρ_{bulk} of cement paste samples were determined at three days of age and were found to be 1.87 g/cm³. The ρ_s , represents the effective density of the solid material, can be obtained using Equ. (6), further reducing the number of internal variables in the expressions for $r(f)$. ρ_s is the composite density of the solid made up of unhydrated cement and the hydration products. The analysis can be simplified considering inter-relations between some of the material parameters [9]

$$c = 1 - r(1 - 1/\beta),$$

from Kozeny-Carman relation

$$\kappa(1 - \beta)^2 / \beta^3 = \kappa_0(1 - \beta_0)^2 / \beta^3 = const. \text{ and } a^2 / \kappa = a_0^2 / \kappa_0 = const. \quad (4)$$

Therefore

$$R_s = R_s(\rho_e, E_e, v_e, \mu_o, \beta, \delta_\mu) \quad (5)$$

The experimental data used in the optimization comprised of the $r(1)$ at three different angles of incidence. The Generalized Reduced Gradient nonlinear optimization scheme was used to minimize an objective function based on squares of the differences [see ref 5 for additional details]. For the numerical inversion, the starting guess for μ_b was taken as 10^5 Pa. The range for δ_μ was initially prescribed to be within $0.01 - 0.3$. It was found that within the prescribed range, there was no influence of δ_μ on the final values of μ_b and β . The solution obtained at a given time was then used as the starting guess for the next time.

Evolution of Porosity in Hydrating Cement Paste

The porosity of cement paste obtained from the ultrasonic measurements are compared with the values obtained from TG weight loss measurements in Fig. 3. The porosity at certain degree of hydration then was calculated using the relations presented by Hansen [9] as

$$\phi(t) = \frac{\rho_{\text{cement}}(w/c) - (1.15 + 0.06\rho_{\text{cement}})\alpha_h(t)}{1 + (\rho_{\text{cement}})(W/C)} \quad (6)$$

where ρ_{cement} is the specific gravity of cement, w/c is the water to cement ratio and α_h is the degree of hydration. The porosities obtained from weight loss measurements agree well with the porosities from poro-elasticity based inversion of ultrasonic data. In addition, the values of porosity determined from TGA measurements for cement paste with w/c equal to 0.5 by Voigt [Ref 10] are also plotted in the Figure. The close agreement between the values of porosity obtained from the poro-elastic equivalent derived from wave reflection measurements and the capillary porosity calculated by applying Power's model to weight loss measurements provides

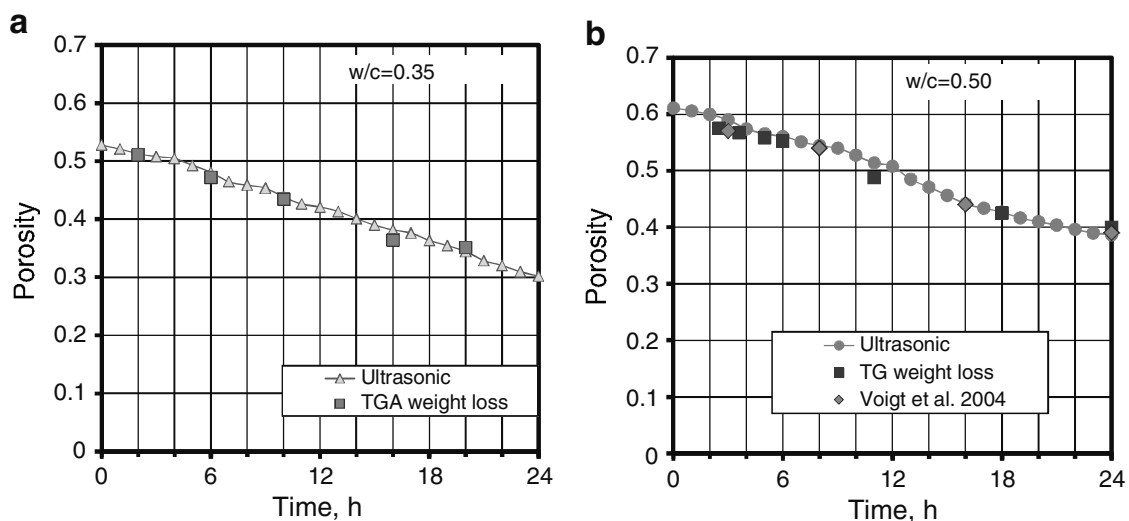


Fig. 3 Porosity from the ultrasonic measurements and the TG weight loss measurements: (a) w/c = 0.35; and (b) w/c = 0.5

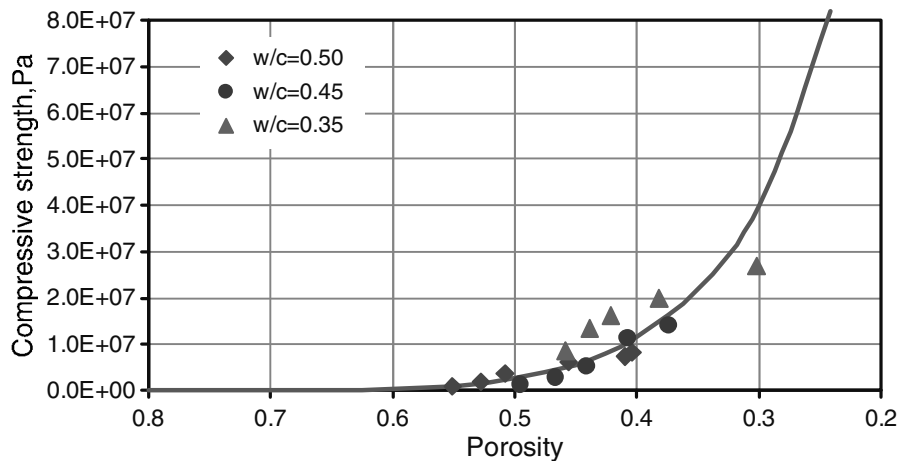


Fig. 4 Relationship between capillary porosity and compressive strength

a validation of the measured porosity. The poro-elastic equivalent for hydrating cement paste, which provides identical response for reflected ultrasonic waves, provides a realistic representation of the cement microstructure at the scale of capillary porosity. This method therefore provides a means for continuous assessment of aging cement microstructure, which can then be related to the development of macroscopic properties.

The influence of porosity on the compressive strength of cement paste is shown in Fig. 4. It can be seen that the relationship between the capillary porosity and the compressive strength is independent of the w/c ratio. This suggests that in hydrating cement paste the strength gain is controlled by the decrease in capillary porosity. While the relationship between the direct measured variable, the reflection factor (r) and the compressive strength is not unique for the different w/c ratios, there is a unique relationship between the microstructural variable derived from the reflection measurement and the compressive strength. It should be noted that the exact relationship between the capillary porosity and compressive strength will depend upon the exact composition of the cementitious material. However, the results presented in Fig. 4 suggest that for a given type of cementitious material, if the relationship between capillary porosity is established, then microstructure based tools for predicting strength gain in hydrating cement based materials can be developed.

Conclusions

An ultrasonic method for continuous, simultaneous measurement of capillary porosity of the material, with time is presented. In hydrating cement pastes, there is a unique relationship between the decrease in porosity and the increase in compressive strength, which does not depend on the w/c ratio of the paste.

References

- [1] Thomas, J.J. and Jennings, H.M., 1999, *Concrete Science and Engineering*, vol. 1: 45–64
- [2] Subramaniam, K.V. and Lee, J., 2006, *Materials and Structures*, 40 no. 3: 301-309
- [3] Bentz, D.P., Garboczi, E.J. and Jensen O.M., 1999 *Cement and Concrete Research*, 29(10): 1663–1671.
- [4] Ye, G. and van Breugel, K. et al. 2003, *Cement and Concrete Research*, vol. 33, no. 2, pp. 233–239.
- [5] Wang, X. and Subramaniam, K.V., 2010, *Cement and Concrete Research*, vol. 40, no. 1, p. 33–44
- [6] Wang, X., and Subramaniam, K.V., 2010, *Ultrasonics*, Vol. 50, no. 7, pp. 726–738
- [7] Stoll, R. and T. Kan 1981, *Journal of Acoustical Society of America*, 70: 149.
- [8] Berryman, J., 1980, *Applied Physics Letters*, 37: 382.
- [9] Hansen, T. C., 1986, *Materials and Structures*, 19 no. 114: 423–436.
- [10] Voigt, T., 2005, Ph.D.Thesis, University of Leipzig, Germany